Initialization of the shooting method via the Hamilton-Jacobi-Bellman approach

Emiliano Cristiani, Pierre Martinon

INSTITUT NATIONAL DE RECHERCHE EN INFORMATIQUE ET EN AUTOMATIQUE

Initialization of the shooting method via the Hamilton-Jacobi-Bellman approach

Emiliano Cristiani — Pierre Martinon

N° 7139

Décembre 2009

ISSN 0249-6399 ISRN INRIA/RR--7139--FR+ENG

INSTITUT NATIONAL
DE RECHERCHE
EN INFORMATIQUE
ET EN AUTOMATIQUE

INRIA

centre de recherche
SACLAY - ÎLE-DE-FRANCE

Initialization of the shooting method via the Hamilton-Jacobi-Bellman approach

Emiliano Cristiani* , Pierre Martinon †

Thème : Modélisation, optimisation et contrôle de systèmes dynamiques
Équipe-Projet Commands

Rapport de recherche n° 7139 — Décembre 2009 — 25 pages

Abstract: The aim of this paper is to investigate from the numerical point of view the possibility of coupling the Hamilton-Jacobi-Bellman (HJB) approach and the Pontryagin's Minimum Principle (PMP) to solve some control problems. We show that an approximation of the value function computed by the HJB method on rough grids can be used to obtain a good initial guess for the PMP method. The advantage of our approach over other initialization techniques (such as continuation or direct methods) is to provide an initial guess close to the global minimum. Numerical tests involving multiple minima, discontinuous control, singular arcs and state constraints are considered. The CPU time for the proposed method is less than four minutes up to dimension four, without code parallelization.

Key-words: optimal control problem, minimum time problem, Pontryagin's minimum principle

* CEMSAC, Fisciano (SA) and IAC-CNR, Rome, Italy
† INRIA and CMAP École Polytechnique, Palaiseau, France

Centre de recherche INRIA Saclay – Île-de-France
Parc Orsay Université
4, rue Jacques Monod, 91893 ORSAY Cedex
Téléphone : +33 1 72 92 59 00

Initialization of the shooting method via the Hamilton-Jacobi-Bellman approach

Résumé : The aim of this paper is to investigate from the numerical point of view the possibility of coupling the Hamilton-Jacobi-Bellman (HJB) approach and the Pontryagin's Minimum Principle (PMP) to solve some control problems. We show that an approximation of the value function computed by the HJB method on rough grids can be used to obtain a good initial guess for the PMP method. The advantage of our approach over other initialization techniques (such as continuation or direct methods) is to provide an initial guess close to the global minimum. Numerical tests involving multiple minima, discontinuous control, singular arcs and state constraints are considered. The CPU time for the proposed method is less than four minutes up to dimension four, without code parallelization.

Mots-clés : optimal control problem, minimum time problem, Pontryagin's minimum principle

1 Introduction

The Hamilton-Jacobi-Bellman (HJB) theory and the Pontryagin's Minimum Principle (PMP) are usually considered two separate worlds although they deal with the same kind of problems. The theoretical connections between the two approaches are well known [11, 7, 8, 9], but coupled usage of the two techniques is not common and not completely explored.
In this paper we will deal with the following controlled dynamics

$$\begin{cases} \dot{y}(t) = f(y(t), u(t)), & t > 0 \\ y(0) = x, & x \in \mathbb{R}^d \end{cases} \tag{1}$$

where the control variable $u(\cdot) \in \mathcal{U} := \{u : \mathbb{R}^+ \to U,\ u \text{ measurable}\}$ and $U \subset \mathbb{R}^m$ $(m \geq 1)$. We will denote by $y_x(t;u)$ the solution of the system (1) starting from the point x with control u. Let $\mathcal{C} \subset \mathbb{R}^d$ be a given *target*. For any given control u we denote by $t_f(x,u)$ the first time the trajectory $y_x(t;u)$ hits $\mathcal{C}$ (we set $t_f(x,u) = +\infty$ if the trajectory never hits the target). We also define a *cost functional* J as

$$J(x,u) := \int_0^{t_f(x,u)} \ell(y_x(t;u), u(t))dt. \tag{2}$$

The final goal is to

$$\text{find } u^* \in \mathcal{U} \text{ such that } J(x,u^*) = \min_{u \in \mathcal{U}} J(x,u) \tag{3}$$

and then to compute the associated optimal trajectory $y_x^*(t;u^*)$. We also define the *value function*

$$\mathcal{T}(x) := J(x,u^*)\,, \quad x \in \mathbb{R}^d.$$

Choosing $\ell \equiv 1$ in (2) we obtain the classical *minimum time* problem.

The HJB approach is based on the Dynamic Programming Principle [3]. It consists in characterizing the value function associated to the control problem by means of a first-order non-linear partial differential equation. Once an approximation of the value function is computed, we can easily reconstruct the optimal control u^* in feedback form and, by a direct integration, the optimal trajectories for any starting point x. The method is greatly advantageous because it is able to reach the global minimum of the cost functional, even if the problem is not convex. The HJB approach allows also to have a global overview of the set of the optimal trajectories and of the reachable set (or capture basin) i.e. the set of the points from which it is possible to reach the target in a given time.

Beside all the advantages listed above, the HJB approach suffers the well known "curse of dimensionality", so in general it is restricted to problems in low dimension ($d \leq 3$).

The PMP approach consists in finding trajectories that satisfy the necessary conditions stated by Pontryagin's Minimum Principle. This is done in practice by searching a zero of a certain shooting function, typically with a (quasi-)Newton method. This method is well known and is used in many applications, see [21, 23, 12] and references therein. The main advantages of this approach lie in its accuracy and its numerical complexity. It is worth to recall

that the dimension of the nonlinear system for the shooting method is usually $2d$, where d is the state dimension. This is in practice quite low for this kind of problem, therefore fast convergence is expected in case of success, especially if the initial guess is close to the right value. Unfortunately, finding a suitable initial guess can be extremely difficult in practice. The algorithm may either not converge at all, or converge to a local minimum of the cost functional.

In this paper we couple the two methods in such a way we can preserve the respective advantages. The idea is to solve the problem via the HJB method on a coarse grid to have in short time a first approximation of the value function and the structure of the optimal trajectory. Then, we use this information to initialize the PMP method and compute a precise approximation of the global minimum. To our knowledge this is the first attempt to exploit the connection between the HJB and PMP theories from the numerical point of view.

Compared to the use of continuation techniques or direct methods to obtain an estimate of the initial costate, the main advantage of the approach presented here is that the HJB method provides an initial guess close to the global minimum. The main limitation is the restriction with respect to the dimension of the state.

We consider some known control problems with different specific difficulties: several local minima, discontinuous control, presence of singular arcs, and state constraints. In all these problems, we show that combining PMP method with HJB approach leads to a very efficient algorithm.

2 Preliminaries

Consider optimal control problems in the general Bolza form, autonomous case, with a fixed or free final time.

$$(P)\begin{cases} \min\ J(x,u) = \int_0^{t_f(x,u)} \ell(y(t),u(t))\ dt & \text{Objective} \\ \dot{y}(t) = f(y(t),u(t)) & \text{Dynamics} \\ u(t) \in U \quad \text{for a.e. } t \in (0,t_f(x,u)) & \text{Admissible Controls} \\ y(0) = x & \text{Initial Conditions} \\ y(t_f(x,u)) \in \mathcal{C} & \text{Terminal Conditions} \end{cases}$$

Here U is a compact set of $\mathbb{R}^m$ and the following classical assumptions are satisfied:

- $f : \mathbb{R}^d \times U \to \mathbb{R}^d$ and $\ell : \mathbb{R}^d \times U \to \mathbb{R}^d$ are continuous, and are of class C^1 with respect to the first variable.
- $\mathcal{C}$ is a closed subset of $\mathbb{R}^d$ for which the property "a vector is normal to $\mathcal{C}$ at a point of $\mathcal{C}$" makes sense. For instance, $\mathcal{C}$ can be described by a finite set of equalities $\{c_i(x) = 0\}_i$ or inequalities $\{c_i(x) \leq 0\}_i$, with the $c_i's$ being of class C^1 and the classical constraint qualification assumptions.

2.1 Pontryagin's Minimum Principle approach

We give here a brief overview of the so called indirect methods for optimal control problems [24, 6, 22]. We introduce the costate p, of same dimension d

as the state x, and define the Hamiltonian

$$H(y,p,u,p_0) = p_0\ell(y,u) + < p, f(y,u) > .$$

Under the assumptions on f and ℓ introduced above, the Pontryagin's Minimum Principle states that if (y_x^*, u^*, t_f^*) is a solution of (P) then there exists $(p_0, p^*) \neq 0$ absolutely continuous such that

$$\dot{y}^*(t) = H_p(y_x^*(t), p^*(t), u^*(t), p_0), \quad y_x^*(0) = x, \tag{4a}$$
$$\dot{p}^*(t) = -H_x(y_x^*(t), p^*(t), u^*(t), p_0), \tag{4b}$$
$$p^*(t_f^*) \perp T_{\mathcal{C}}(y_x^*(t_f^*)), \tag{4c}$$
$$u^*(t) = \arg\min_{v\in U} H(y_x^*(t), p^*(t), v, p_0) \quad \text{for a.e. } t \in [0, t_f^*], \tag{4d}$$

where $T_{\mathcal{C}}(\xi)$ denotes the contingent cone of $\mathcal{C}$ at ξ. Moreover, if the final time t_f^* is not fixed and is an optimal time, then we have the additional condition:

$$H(y_x^*(t), p^*(t), u^*(t), p_0) = 0, \quad \text{for } t \in (0, t_f^*). \tag{5}$$

Two common cases are $\mathcal{C} = \{y_f\}$ with $p^*(t_f^*)$ free, and $\mathcal{C} = \mathbb{R}^d$ with $p(t_f^*) = 0$.

Now we assume that minimizing the Hamiltonian provides the control as a function γ of the state and costate. For a given value of $p(0)$, we can integrate (x,p) by using the control $u = \gamma(x,p)$ on $[0, t_f]$. We define the shooting function S that maps the unknowns $p(0)$ to the value of the final and transversality conditions at $(x(t_f), p(t_f))$. Finding a zero of S gives a trajectory (x,u) that satisfies the necessary conditions for the problem (P). This is typically done in practice by applying a (quasi-)Newton method.

Remark 2.1 *The multiplier p_0 could be equal to 0. In that case, the PMP is said anormal, its solution (y^*, u^*, p^*) corresponds to a "singular" extremal which does not depend on the cost function ℓ. Several works have been devoted to the existence (or nonexistence) of such extremal curves [4, 10]. For numerics, in general we assume that $p_0 \neq 0$ which leads to solve the PMP system with $p_0 = 1$. In the sequel, we will always assume that we are in the normal case ($p_0 = 1$).*

Singular arcs. A singular arc occurs when minimizing the Hamiltonian fails to determine the optimal control u^* on a whole time interval. The typical context is when H is linear with respect to u, with an admissible set of controls of the form $U = [u_{low}, u_{up}]$. In this particular case, the function $(x,u,p) \longmapsto H_u(x,u,p)$ does not depend on the control variable. We define the switching function $\psi(x,p) = H_u(x,u,p)$ and have the following bang-bang control law:

$$\begin{cases} \text{if } \psi(x,p) > 0 & \text{then } u^* = u_{low} \\ \text{if } \psi(x,p) < 0 & \text{then } u^* = u_{up} \\ \text{if } \psi(x,p) = 0 & \text{then switching or singular control.} \end{cases}$$

A singular arc then corresponds to a time interval where the switching function ψ is zero. The usual way to obtain the singular control is to differentiate ψ with respect to t until the control explicitly appears, which leads to solving an equation of the form $\psi^{(2k)}(x,p) = 0$, see [6]. This step can be quite difficult in practice,

depending on the problem. Moreover, it is also required to make assumptions about the control structure, more precisely to fix the number of singular arcs. Each expected singular arc adds two shooting unknowns (t_{entry}, t_{exit}), with the corresponding junction conditions $\psi(t_{entry}) = \dot{\psi}(t_{entry}) = 0$ or alternately $\psi(t_{entry}) = \psi(t_{exit}) = 0$. The problem studied in section 4.3 presents such a singular arc.

State constraints. We consider a state variable inequality constraint $g(x(t)) \leq 0$. We denote by q the smallest order such that $g^{(q)}$ depends explicitly on the control u; q is called the order of the constraint g. The Hamiltonian is defined with an additional term for the constraint

$$H(x, p, u) = \ell(x, u) + < p, f(x, u) > +\mu g^{(q)}(x, u)$$

with the sign condition

$$\begin{cases} \mu = 0 & \text{if } g < 0 \\ \mu \geq 0 & \text{if } g = 0. \end{cases}$$

When the constraint is inactive we are in the same situation as for an unconstrained problem. Over a constrained arc where $g(x) = 0$, we obtain the control from the equation $g^{(q)}(x, u) = 0$, and μ from the equation $H_u = 0$. As in the singular arc case, we need to make assumptions concerning the control structure, namely the number of constrained arcs. Each expected constrained arc adds two shooting unknowns (t_{entry}, t_{exit}) with the Hamiltonian continuity as corresponding conditions. We also have the so called tangency condition at the entry point

$$N(x(t_{entry})) = (g(x(t_{entry})), \dots, g^{(q-1)}(x(t_{entry}))) = 0,$$

with the costate discontinuity

$$p(t^+_{entry}) = p(t^-_{entry}) - \pi N_{x\ |t_{entry}}$$

where $\pi \in \mathbb{R}^q$ is another multiplier yielding to an additional shooting unknown.

Remark 2.2 *The tangency condition can also be enforced at the exit time, in this case the costate jump occurs at the exit time as well.*

2.2 Hamilton-Jacobi-Bellman approach

Consider the value function $\mathcal{T} : \mathbb{R}^d \to \mathbb{R}$, which maps every initial condition $x \in \mathbb{R}^d$ to the minimal value of the problem (P). It is well known (see for example [1] for a comprehensive introduction) that the value function $\mathcal{T}$ satisfies a Dynamic Programming Principle and the Kružkov transform of $\mathcal{T}$, defined by

$$v(x) := 1 - e^{-\mathcal{T}(x)}$$

is the unique solution of the following HJB equation, in *viscosity* sense [1]:

$$\begin{cases} v(x) + \sup_{u \in U} \{-f(x, u) \cdot Dv(x) - \ell(x, u) + (\ell(x, u) - 1)v(x))\} = 0 & x \in \mathbb{R}^d \backslash \mathcal{C} \\ v(x) = 0 & x \in \mathcal{C}. \end{cases} \tag{6}$$

Obtaining a numerical approximation of the function v is a difficult task mainly because v is not always differentiable. Several numerical schemes have been studied in the literature. In this paper we will use a first-order semi-Lagrangian (SL) scheme, we refer to [13, 14] for a survey on these kind of schemes. This choice is motivated by the fact that SL scheme seems the best one in order to approximate the gradient of the value function, this being our goal as we will see in the next section. We fix a (numerical) bounded domain $\Omega \supset \mathcal{C}$ and we introduce in it a regular grid $G = \{x_i, i = 1, \dots, N_G\}$ where N_G is the total number of nodes. We denote by $\widetilde{v}(x; h, k, \Omega)$ the fully discrete approximation of v, h and k being two discretization parameters (the first one can be interpreted as a time step to integrate along characteristics and the second one is the usual space step). We impose state constraint boundary conditions on $\partial\Omega$. The discrete version of (6) is

$$\begin{cases} \widetilde{v}(x_i) = \widetilde{H}[\widetilde{v}](x_i) & x_i \in (\Omega \backslash \mathcal{C}) \cap G \\ \widetilde{v}(x_i) = 0 & x \in \mathcal{C} \cap G \end{cases} \tag{7}$$

where

$$\widetilde{H}[\widetilde{v}](x_i) := \min_{u \in U} \{\mathbb{P}_1\big(\widetilde{v}; x_i + hf(x_i, u)\big) + h\ell(x_i, u)(1 - \widetilde{v}(x_i))\} \tag{8}$$

and $\mathbb{P}_1\big(\widetilde{v}; x_i + hf(x_i, u)\big)$ denotes the value of $\widetilde{v}$ at the point $x_i + hf(x_i, u)$ obtained by linear interpolation using the known values of $\widetilde{v}$ on G (note that the point $x_i + hf(x_i, u)$ is not in general sitting on the grid). The numerical scheme consists in iterating

$$\widetilde{v}^{(n+1)} = \widetilde{H}[\widetilde{v}^{(n)}] \qquad n = 1, 2, \dots \tag{9}$$

until convergence, starting from $\widetilde{v}^{(0)}(x_i) = 0$ on $\mathcal{C}$ and 1 elsewhere. To accelerate the convergence we use the Fast Sweeping technique [27]. The function $\widetilde{v}$ is then extended to the whole space by linear interpolation. Once the function $\widetilde{v}$ is computed, we get easily the corresponding approximation $\widetilde{\mathcal{T}}$ of $\mathcal{T}$, and then the optimal control law in feedback form, see [13, 14] for details.

It is useful to note that the equation (6) can also model a front (interface) propagation problem. Following this interpretation, the boundary of the target $\partial\mathcal{C}$ is the front at initial time $t = 0$, and the level set $\{x : \mathcal{T}(x) = t\}$ represents the front at any time $t > 0$.

3 Coupling HJB and PMP

3.1 Main connection

It is known [7] that for a general control problem with free end-point, if the value function is differentiable at some point $x \in \mathbb{R}^d$ then it is differentiable along the optimal trajectory starting at x. Actually, *the gradient of the value function is equal to the costate of the Pontryagin's principle.*
In the context of minimum time problems (with target constraint), the link between the minimum time function and the Pontryagin's principle has been also investigated in several papers [9, 8], proving the same connection.

Once the value function $\mathcal{T}$ is computed by solving the HJB equation, we approximate $D\mathcal{T}(x)$ (x being the starting point) by standard first-order finite differences, and then we use it as initial guess for $p(0)$.

In the case $\mathcal{T} \notin C^1(\mathbb{R}^d)$ it is proved in [8] that a connection between the two approaches still exists. More precisely, under some additional assumptions, we have

$$p^*(t) \in D^+\mathcal{T}(y_x^*(t)) \quad \text{for } t \in [0, \mathcal{T}(x)],$$

where $D^+\mathcal{T}(x)$ is the *superdifferential* of $\mathcal{T}$ at x defined by

$$D^+\mathcal{T}(x) := \left\{ \eta \in \mathbb{R}^d : \limsup_{y \to x} \frac{\mathcal{T}(y) - \mathcal{T}(x) - \eta \cdot (y - x)}{|y - x|} \leq 0 \right\}. \tag{10}$$

In the rest of this section we assume that $D^+\mathcal{T}(x) \neq \emptyset$. It is plain that we can not use finite difference approximation in order to compute $p(0)$ at the points where the value function $\mathcal{T}$ is not differentiable. Rather than that, we will try to approximate the direction ξ^* which is orthogonal to the level sets of $\mathcal{T}$, pointing toward the direction of maximal decrease. This direction, in the case when $\mathcal{T}$ is differentiable, is given by:

$$\xi^* = -D\mathcal{T}(x). \tag{11}$$

Here, we compute an approximation of ξ^* as:

$$\xi^* = \arg \min_{\xi \in B(0,1)} \frac{\mathcal{T}(x + \delta\xi) - \mathcal{T}(x)}{\delta}, \tag{12}$$

where $\delta > 0$ is a small positive parameter, and $B(0,1)$ denotes the ball in $\mathbb{R}^d$ centered at 0 with radius 1.

Let us explain on a simple example why we choose the definition (12). Consider the case $\mathcal{C} = \{(3,0)\} \cup \{(-3,0)\}$, $\ell \equiv 1$, $f = u$ and $U = B(0,1)$ (eikonal equation). On the line $\{x = 0\}$ the function $\mathcal{T}$ is not differentiable (see Fig. 1-left). This line corresponds to a zone where two globally optimal trajecto-

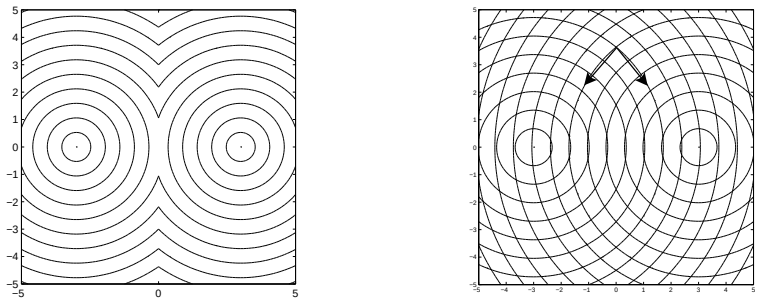

Figure 1: two crossing fronts with and without superimposition. Arrows correspond to the (two) vector(s) ξ^*

ries are available. Following the front propagation interpretation (see end of

section 2.2) here we have two fronts which hit each other at the line $\{x = 0\}$. The viscosity solution of the HJB equation selects automatically the first arrival time so we never see the two crossing fronts, but we could in principle follow the propagations of the two fronts separately (see Fig. 1-right). Considering the two fronts separately, by means of (12), we can easily approximate the two directions ξ_1^* and ξ_2^* of maximal decrease of the function $\mathcal{T}$ (and then the "two gradients" $-\xi_1^*$ and $-\xi_2^*$ of $\mathcal{T}$) using only the value function $\mathcal{T}$.

In the present example, focusing on the point $(0, 0)$, we easily compute the two directions of maximal decrease as $(-1, 0)$ and $(1, 0)$. It is easy to show that these two vectors coincide with the two "extremal" vectors in $D^+\mathcal{T}(x)$, namely the vectors η verifying

$$\limsup_{y \to x} \frac{\mathcal{T}(y) - \mathcal{T}(x) - \eta \cdot (y - x)}{|y - x|} = 0. \tag{13}$$

Although this relationship is not true for every function $\mathcal{T}$ such that $D^+\mathcal{T}(x) \neq \emptyset$, it is easy to see that it is true whenever the curve of non-differentiability is due to the collision of two or more fronts (as in Problem 1, Section 4.1).

In this paper, we propose to investigate numerically the relevance of using the HJB approach to compute $-\xi^*$ and then using it as initial guess for the initial costate $p(0)$ in the shooting method.

3.2 Convergence of $D\mathcal{T}$

Many papers (see for example [2, 26] in the context of differential games) investigated the convergence of the approximate value function $\widetilde{v}(\cdot\,; h, k, \Omega)$ to the exact solution v when the parameters h, k tend to zero and Ω tends to $\mathbb{R}^d$. These results were quite difficult to be obtained because the function v is not in general differentiable.
Let us denote by $\widetilde{D} = (\widetilde{D}_1, \ldots, \widetilde{D}_d)$ the discrete gradient computed by centered finite differences with step $z > 0$

$$\widetilde{D}_i\mathcal{T}(x) := \frac{\mathcal{T}(x + ze_i) - \mathcal{T}(x - ze_i)}{2z}, \quad i = 1, \ldots, d$$

where $\{e_i\}_{i=1,\ldots,d}$ is the standard basis of $\mathbb{R}^d$.
To our purposes we have to go further proving the convergence of $\widetilde{\mathcal{T}}(\cdot; h, k, \Omega) = -\ln(1 - \widetilde{v}(\cdot\,; h, k, \Omega))$ and then the convergence of $\widetilde{D}\widetilde{\mathcal{T}}(\cdot\,; h, k, \Omega)$ because the latter will be used by the PMP method as initial guess.
Let us assume that $k = C_1 h$ for some constant C_1. Given a generic estimate of the form

$$\|\widetilde{v}(\cdot\,; h, \mathbb{R}^d) - v(\cdot)\|_{L^\infty(\mathbb{R}^d)} \leq Ch^\alpha, \quad C, \alpha > 0 \tag{14}$$

we have the following

Theorem 3.1 *Assume that $\mathcal{T} \in C^1(\Omega)$ and there exists $\mathcal{T}_{max} > 0$ such that*

$$0 \leq \mathcal{T}(x) \leq \mathcal{T}_{max} \quad \textit{for all } x \in \Omega.$$

Let us define

$$E(x) := \|\widetilde{D}\widetilde{\mathcal{T}}(x; h, \Omega) - D\mathcal{T}(x)\|_\infty.$$

Then there exists $\Omega' \subset \Omega$ such that

$$\|E(\cdot)\|_{L^\infty(\Omega')} = O(h^\alpha/z) + O(z^2) \quad \textit{for } h, z \to 0.$$

For the SL scheme we use here, an estimate of the form (14) in the particular case $\ell \equiv 1$ (under assumptions weaker than those used in Theorem 3.1) can be found in [26]. The proof of the theorem is postponed in the Appendix.

4 Numerical experiments

We have tested the feasibility and relevance of combining the HJB and PMP methods on four optimal control problems. Each of these problems highlights a particular difficulty from the control point of view.

Problem 1 (section 4.1) is a simple minimum time target problem in dimension two presenting local and global minima. We will see in this example that the shooting method is very sensitive with respect to the initial guess (as usual). When initialized by using the HJB approach, shooting method recovers the optimal solution.

Problem 2 (section 4.2) is a controlled Van der Pol oscillator, also of dimension two, with control switchings.

Problem 3 (section 4.3) is the well-known Goddard problem with singular arcs, in the one-dimensional case (total state dimension is three).

Problem 4 (section 4.4) is another simple minimum time target problem in dimension four, with a first-order state constraint.

Details for HJB implementation. The algorithm is written in C++ and it runs on a PC with an Intel Core 2 Duo processor at 2.00 GHz and 4GB RAM. Note that the code is not parallelized. The indicated CPU time is the time needed for the computation of the value function and saving the result on file. The time needed to reconstruct the optimal trajectory is not considered (is almost 0).
The numerical domain Ω is discretized by a regular grid with $N_1 \times \ldots \times N_d$ nodes. The set of admissible controls U is discretized in N_C equispaced discrete controls $u_1, \ldots, u_{N_C}$. The stop criterion for the fixed point iterations (9) is $\|\widetilde{v}^{(n+1)} - \widetilde{v}^{(n)}\|_{L^\infty(\Omega)} < \varepsilon = 1e-5$.

Details for PMP implementation. The shooting method is written in Fortran 90 and runs on a PC with an Intel Core 2 Duo processor at 2.33 GHz and 2GB RAM. We used the SHOOT[1] software which implements a shooting method with the HYBRD [19] solver. For the four problems studied we set the ODE integration method to a basic 4th-order Runge-Kutta with 100 steps.

4.1 Minimum time target problem

The first example illustrates how a local solution can affect the shooting method. We consider a simple minimum time problem where we want to reach a certain position on the plane by controlling the angle of the speed. We choose the velocity in order to create multiple minima of the cost functional.

[1] http://www.cmap.polytechnique.fr/~martinon/

$$(P_1)\begin{cases} \min\ t_f \\ \dot{y}_1(t) = c(y_1(t), y_2(t))\cos(u(t)) \\ \dot{y}_2(t) = c(y_1(t), y_2(t))\sin(u(t)) \\ u(t) \in [0, 2\pi) \quad \text{for a.e. } t \in (0, t_f) \\ y(0) = x = (-2.5, 0) \\ y(t_f) = (3, 0) \end{cases}$$

with

$$c(y_1, y_2) = \begin{cases} 1 & \text{if } y_2 \leq 1 \\ (y_2 - 1)^2 + 1 & \text{if } y_2 > 1. \end{cases}$$

Due to the expression of c, we have at least two minima. The simplest one corresponds to a straight line trajectory $(-)$ along the y_1 axis with $y_2 = 0$. The other one has a curved trajectory $(\cap)$ that takes advantage of the larger values of y_2.

4.1.1 PMP and shooting method

We first try to solve the problem with the PMP and the shooting method. Therefore we seek a zero of the shooting function defined by

$$S_1 : \begin{pmatrix} t_f \\ p_1(0) \\ p_2(0) \end{pmatrix} \mapsto \begin{pmatrix} y_1(t_f) - 3 \\ y_2(t_f) \\ p_3(t_f) - 1 \end{pmatrix}.$$

Global and local solutions. Depending on the starting point, the shooting method can converge to a local or global solution (Fig. 2). The more common local solution is the straight line trajectory from x to $\mathcal{C} := \{(3, 0)\}$, with a constant control $u = 0$ and a final time $T_{local} = 5.5$. The global solution has an arch shaped trajectory that benefits from the higher speed for increasing values of y_2, with a final time $t_f^* = T_{global} = 4.868$.

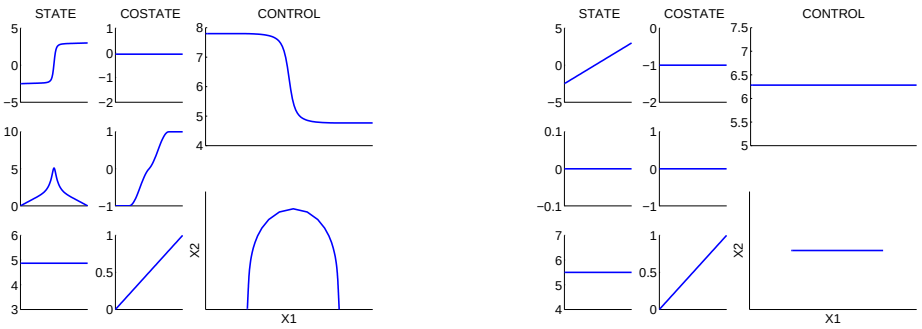

Figure 2: (P_1) - Global solution (curved trajectory) and local solution (straight trajectory) found by the shooting method.

Sensitiveness with respect to the starting point. Even for this simple problem, the shooting method is very sensitive to the starting point. Numerical tests indicate that it converges in most cases to local solutions. We run the shooting method with a batch of 441 values of $p(0) \in [-10, 10]^2$ on a 21×21 grid, with different starting guesses for the final time (Fig. 3). We observe that for the batch with the $t_f = 1$ initialization, 11% of the shootings converge to the global solution, 60% to the straight line local solution, and 24% to another local solution with an even worse final time ($t_f = 6.06$). For the batch with the $t_f = 10$ initialization, 9% of the shootings converge to the global solution, and 50% and 29% to the two local solutions. Obviously, just taking a random starting point is not a reliable way to find the global solution.

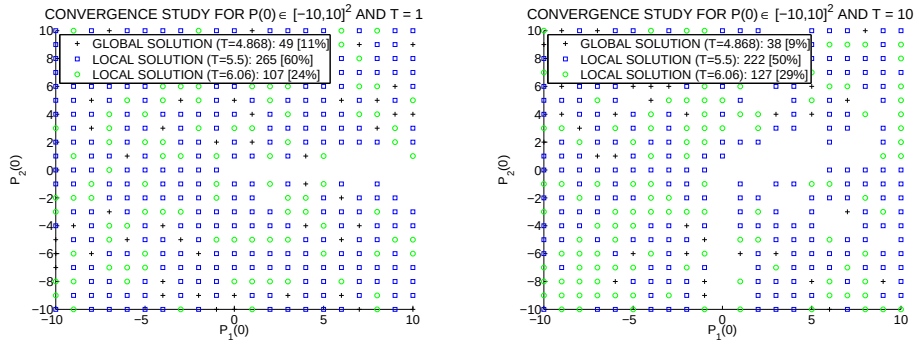

Figure 3: (P_1) - Convergence to the global solution from a random initialization is hazardous due to the presence of a local solution.

4.1.2 Solving the problem with the HJB approach

In Fig. 4, we show the level sets of the minimum time function $\mathcal{T}$ associated to the control problem (P_1). These level sets are obtained by solving numerically the HJB equation. As it can be easily seen in Fig. 4, the minimum time function is not differentiable everywhere. The curve of the discontinuity of the gradient represents here the set of the initial points associated to two optimal trajectories.

4.1.3 Coupling the HJB and PMP approaches

We now use the data provided by the HJB approach to obtain a starting point close to the global solution. The HJB solution provides an estimate of the final time, and also an approximation of the costate $p(0)$ by computing a direction of maximal decrease of the minimum time function at $y(0) = x$. In Table 1, we summarize the results obtained by solving the HJB equation on several grids, and give the obtained minimal time to reach the target starting from the position $x = (-2.5, 0)$. As we can see, even on a coarse grid (25×25 nodes), we obtain a good approximation of $p(0)$ in a very short time (the CPU times in Table 1 include the numerical resolution of the HJB equation and the computation of $p(0)$). As we expected, the shooting method immediately converges to the global solution when using the starting point obtained from the HJB method (Table 2).

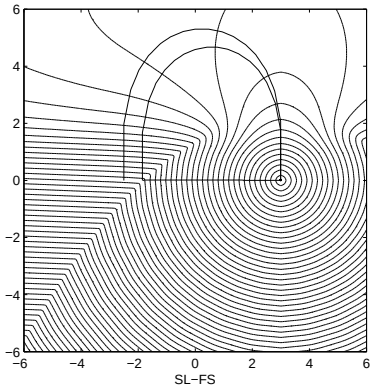

Figure 4: (P_1) - Level sets of the minimum time function $\mathcal{T}$, the optimal trajectory starting from $(-2.5, 0)$ and the two optimal trajectories starting from $(-1.835, 0)$.

nodes	N_C	$-\xi^*$	t_f^*	CPU time (sec)
25×25	16	(-0.049, -1.000)	4.895	0.08
50×50	16	(-0.048, -1.000)	4.895	0.37
200×200	32	(-0.051, -1.000)	4.878	20.25

Table 1: (P_1) - HJB approach: the optimal minimal time starting from $x = (-2.5, 0)$, and the approximation $-\xi^*$ of the initial costate associated to the optimal trajectory

Initialization from HJB	$t_f^* = 4.89$	$-\xi^* = (-0.05, -1)$
Solution by PMP	$t_f^* = 4.868$	$p(0) = (-5.552 \times 10^{-2}, -9.985 \times 10^{-1})$

Table 2: (P_1) - Initialization from HJB and solution from PMP.

We can check that the convergence of the shooting method is much better in a neighbourhood of the HJB initialization. Compared to the previous grid with $p(0) \in [-10, 10]^2$, we test initial points with $p(0) \in [-0.1, 0] \times [-2, 0]$, which corresponds to a 100% range around the HJB initialization $-\xi^* = (-0.05, -1)$; we also set $t_f = 4.89$. This time the shooting method finds the global solution for 76% of the points, and only 12% and 9% for the local solutions (Fig. 5).

In Table 3 (see also Fig. 4), we consider the case of a starting point very close to the curve where the minimal time function is not differentiable: $x = (-1.835, 0)$. Here the computation of $p(0)$ by HJB gives the two directions $p(0) = (-0.05, -1.00)$ and $p(0) = (-0.99, 0.00)$. Using these two values to initialize the shooting method, we obtain the two distinct solutions with the "cap" and "straight" trajectories (Table 4). For this problem, the starting points where the minimal time function is not differentiable correspond to the case

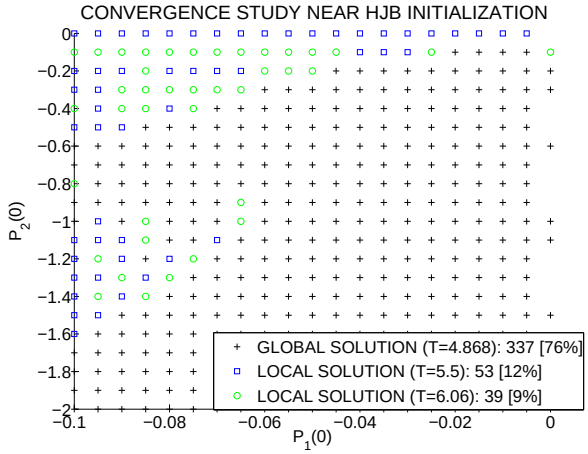

Figure 5: (P_1) - Convergence to the global solution is much easier near the HJB initialization.

where the local ("straight") solution becomes global and has the same minimal time as the global ("cap") solution. Notice that here the minimal time function remains differentiable along each trajectory. We will see in section 4.2 a different case of non differentiability for the value function.

nodes	N_C	$-\xi^*$	t_f^*	CPU time (sec)
300×300	32	(-0.05,-1.00) and (-0.99,0.00)	4.84	39.98

Table 3: (P_1) - HJB approach for an initial position $x = (-1.835, 0)$.

	t_f^*	$p(0)$
HJB	4.84	$(-0.05, -1)$ and $(-0.99, 0)$
PMP $(\cap)$	4.8246	$(-7.67 \times 10^{-2}, -9.97 \times 10^{-1})$
PMP $(-)$	4.835	$(-1, -6.2137 \times 10^{-16})$

Table 4: (P_1) - Local solution becomes global for a starting point where the minimal time function is not differentiable.

4.2 Van der Pol oscillator

The second test problem is a controlled Van der Pol oscillator. Here we want to reach the steady state $(y_1, y_2) = (0, 0)$ in minimum time. It is well known that the optimal trajectories, for this problem, are associated to bang-bang control

variables.

$$(P_2)\begin{cases} \min\ t_f \\ \dot{y}_1(t) = y_2(t) \\ \dot{y}_2(t) = -y_1(t) + y_2(t)(1 - y_1(t)^2) + u(t) \\ u(t) \in [-1, 1] \\ y(0) = x = (1, -0.8) \\ y(t_f) = (0, 0) \end{cases}$$

4.2.1 PMP and shooting method

Here, the Hamiltonian is linear with respect to u, therefore we have a bang-bang control with the switching function $\psi(x, p) = H_u(x, p, u) = p_2$.

The shooting function is defined by

$$S_2 : \begin{pmatrix} t_f \\ p_1(0) \\ p_2(0) \end{pmatrix} \mapsto \begin{pmatrix} y_1(t_f) \\ y_2(t_f) \\ p_3(t_f) - 1 \end{pmatrix}.$$

We test the shooting method with the same initial points as for problem (P_1). The convergence results are even worse in this case: for the $t_f = 1$ initialization, only 9% of the shootings converge to the global solution, and 0.5% for the $t_f = 10$ initialization.

4.2.2 Solving the problem with the HJB approach

Here we use the HJB approach to compute the minimal time function. In Fig. 6, we show the numerical solution obtained by carrying out computations on a 200×200 grid and $N_C = 2$.

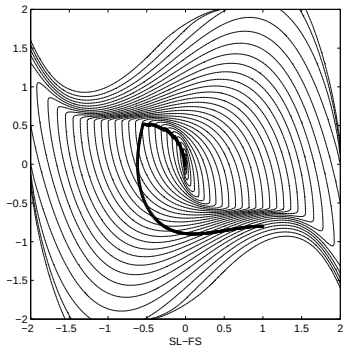

Figure 6: (P_2) - Level sets of function $\mathcal{T}$ and the optimal trajectory starting from $(1, -0.8)^{\mathsf{T}}$.

4.2.3 Coupling the HJB and PMP approaches

The numerical solution of the HJB equation provides some useful data, namely an approximation of the final time t_f and an initial costate $p(0)$. This information is used here to start the shooting algorithm. Once again, the HJB

initialization gives an immediate accurate convergence to the optimal solution, see Table 5 and Fig. 7. In this example, the control discontinuities hinder the

Initialization from HJB	$t_f^* = 4.2$	$-\xi^* = (1.2, -4.2)$
Solution from PMP	$t_f^* = 3.837$	$p(0) = (1.249, -3.787)$

Table 5: (P_2) - Initialization from HJB and solution from PMP.

convergence by testing different integration schemes for the state and costate pair (x, p). Using a fixed step integrator (4th order Runge-Kutta) without any precautions gives a very poor convergence with a norm of $\approx 10^{-3}$ for the shooting function. Using either a variable step integrator (DOPRI, see [17]) or a switching detection method for the fixed step integrator (see [15]) we get much better results ($\approx 10^{-11}$ for the shooting function norm).

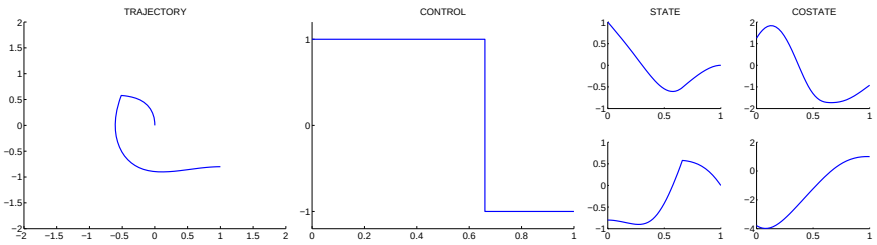

Figure 7: (P_2) - Solution with one switch for the Van der Pol oscillator (shooting method).

We now test two starting points for which the minimal time function is not differentiable. In the previous problem the non differentiability was caused by a local solution becoming global (following the front propagation interpretation, two fronts are hitting). Here the non differentiability has a different nature. It can not be seen as the curve of collision between fronts, and corresponds to the points where the control switches between -1 and $+1$. Taking such a starting point we have a solution with a constant control $u = \pm 1$ and no switches. We test the two starting points $x = (1.5, -0.67)$ and $x = (1, -0.57)$ that are close to the non differentiable curve (see Fig. 6). Computation of ξ^* is performed as before in the case $\mathcal{T}$ is not differentiable. We observe that the shooting method finds solutions with a switch immediately after the initial time or just before the final time. Here the HJB initialization is not as close to the initial costate $p(0)$, but is sufficient to obtain convergence. Also, the minimum times given by HJB are still close to the exact ones (Table 6).

4.3 Goddard problem

The third example is the well-known Goddard problem (see for instance [16, 18, 20, 28, 25, 5]), to illustrate the case of singular arcs. This problem models the ascent of a rocket through the atmosphere, and we restrict here ourselves to vertical (monodimensional) trajectories. The state variables are the altitude, speed and mass of the rocket during the flight, for a total dimension of 3. The

x	method	$p(0)$	t_f
$(1.5, -0.67)$	HJB	$(1.62, -0.87)$	2.96
	PMP	$(1.487, 2.309 \times 10^{-3})$	2.9594
$(1, -0.57)$	HJB	$(1.96, -0.10)$	2.2
	PMP	$(1.715, 1.111 \times 10^{-2})$	2.1351

Table 6: (P_2) - Solutions with no switches for starting point where the value function is not differentiable.

rocket is subject to gravity, thrust and drag forces. The final time is free, and the objective is to reach a certain altitude with a minimal fuel consumption.

$$(P_3) \begin{cases} \min\ J(u) = \int_0^{t_f} bT_{max}u \\ \dot{r} = v \\ \dot{v} = -\frac{1}{r^2} + \frac{1}{m}(T_{max}u - D(r,v)) \\ \dot{m} = -bT_{max}u \\ u(t) \in [0,1] \\ r(0) = 1,\ v(0) = 0, m(0) = 1, \\ r(t_f) \geq 1.01 \end{cases}$$

with the parameters used for instance in [20]: $b = 7$, $T_{max} = 3.5$ and drag $D(r,v) = 310v^2e^{-500(r-1)}$.

4.3.1 PMP and shooting method

As for (P_2), the Hamiltonian is linear with respect to u, and we have a bang-bang control with possible switchings or singular arcs. The switching function is $\psi(x,p) = H_u(x,p,u) = T_{max}((1-p_m)b + \frac{p_v}{m})$, and the singular control can be obtained by formally solving $\ddot{\psi} = 0$. The main difficulty, however, is to determine the structure of the optimal control, namely the number and approximate location of singular arcs. The HJB approach is able to provide such information, in addition to the initial costate $p(0)$. Assuming for instance one interior singular arc, the shooting function is defined by

$$S_3 : \begin{pmatrix} t_f, p_1(0), p_2(0), p_3(0) \\ t_{entry} \\ t_{exit} \end{pmatrix} \mapsto \begin{pmatrix} r(t_f) - 1.01, p_2(t_f), p_3(t_f), p_4(t_f) \\ \psi(x(t_{entry}), p(t_{entry})) \\ \dot{\psi}(x(t_{entry}, p(t_{entry})) \end{pmatrix}.$$

4.3.2 Solving the problem with the HJB approach

Goddard problem is also hard to solve with the HJB approach, specially because the computation of the value function needs a huge number of iterations to converge and the solution is quite sensible to the choice of the numerical box Ω in which the value function is computed. In Fig. 8,

we show the optimal trajectory and the optimal control computed by HJB on a rough grid. As we can see, the HJB approach does not give a good approximation of the optimal control (vertical lines correspond to strong oscillations of the solution). The HJB formulation can suggest not only the values for $p(0)$ and t_f, but also the location of the singular arc.

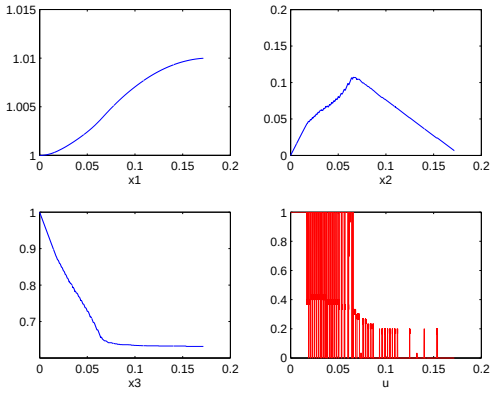

Figure 8: (P_3) - Goddard problem, solution by HJB approach (first line: altitude and velocity. Second line: mass and control).

4.3.3 Coupling the HJB and PMP approaches

We now try to initialize the shooting method directly from the results of the HJB approach. As for problems (P_1) and (P_2), the HJB solution provides an estimate of the final time t_f^* and initial costate $p(0)$. Moreover, examining the state variables on the HJB solution also gives a good idea of the structure of the control: the change of slope on the speed clearly visible in Fig. 8 indicates an interior singular arc at $(t_{entry}, t_{exit}) \approx (0.02, 0.06)$. Once again we obtain a quick convergence to the correct solution with the expected singular arc (Table 7 and Fig. 9)).

	t_f^*	(t_{entry}, t_{exit})	$-\xi^*$ and $p(0)$
Initialization from HJB	0.17	$(0.02, 0.06)$	$(-7.79, -0.31, 0.04)$
Solution from PMP	0.1741	$(0.02351, 0.06685)$	$(-7.275, -0.2773, 0.04382)$

Table 7: (P_3) - Initialization from HJB and solution from PMP.

4.4 Minimum time target problem with a state constraint

This fourth example aims to illustrate the case of a state constraint, as well as a four-dimensional problem for the HJB approach. We chose a simple problem where we want to move a point on the plane, from a steady initial position to a target position, with a null initial and final speed. The control is the direction of acceleration, and the objective is to minimize the final time. We add a state constraint which limits the velocity of the point along the x-axis.

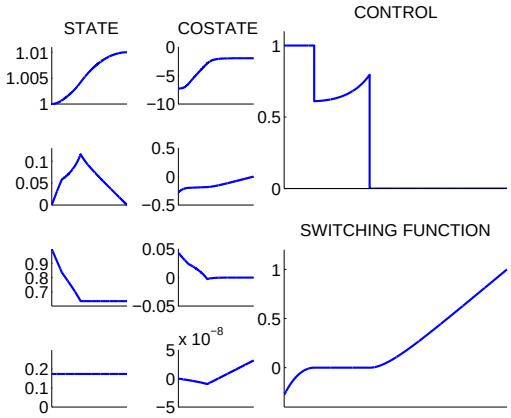

Figure 9: (P_3) - Goddard problem, solution by PMP method.

$$(P_4)\begin{cases} \min\ J(x,u) = t_f \\ \dot{y}_1 = y_3 \\ \dot{y}_2 = y_4 \\ \dot{y}_3 = \cos(u) \\ \dot{y}_4 = \sin(u) \\ u(t) \in [0, 2\pi) \\ y(0) = x = (-3, -4, 0, 0) \\ y(t_f) = (3, 4, 0, 0) \\ y_3(t) \leq 1 \quad t \in (0, t_f) \end{cases}$$

Let us write the state constraints as $g(y(t)) \leq 0$, with g defined by $g(y) = y_3 - 1$. The control appears explicitly in the first time derivative of g, so the constraint is of order 1, and we have:

$$\dot{g}(y(t)) = \cos(u(t)), \quad g_y(y) = (0, 0, 1, 0).$$

When the constraint is not active, minimizing the Hamiltonian gives the optimal control u^* via

$$(\cos(u^*), \sin(u^*)) = -\frac{(p_3, p_4)}{\sqrt{p_3^2 + p_4^2}}.$$

Over a constrained arc where $g(x) = 0$, the equation $\dot{g}(x, u) = 0$ and minimizing the Hamiltonian H leads to

$$u^* = -sign(p_4)\frac{\pi}{2}.$$

Then the condition $H_u = 0$ gives the value for the constraint multiplier $\mu = -p_3$. At the entry point we have a jump condition for the costate:

$$p(t_{entry}^+) = p(t_{entry}^-) - \pi_{entry}\ g_x,$$

with $\pi_{entry} \in \mathbb{R}$ an additional shooting unknown. Compared to the unconstrained problem, we have three more unknowns t_{entry}, t_{exit} and π_{entry}. The corresponding equations are the Hamiltonian continuity at t_{entry} and t_{exit} (which

boils down to $p_3 = 0$), and the tangential entry condition $g(x(t_{entry})) = 0$. The shooting function is defined by

$$S_4 : \begin{pmatrix} t_f \\ p_{1\ldots4}(0) \\ t_{entry}, t_{exit}, \pi_{entry} \end{pmatrix} \mapsto \begin{pmatrix} p_5(t_f) - 1 \\ y_{1\ldots4}(t_f) - (-3, -4, 0, 0) \\ p_3(t_{entry}), p_4(t_{entry}), g(y(t_{entry})) \end{pmatrix}.$$

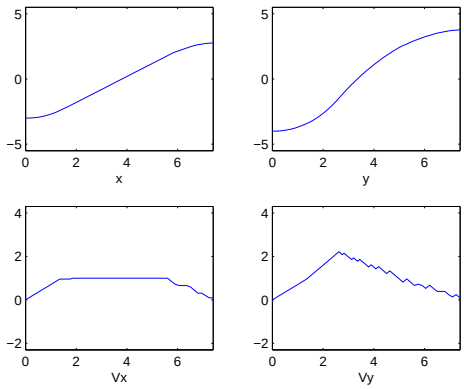

Figure 10: (P_4) - Solution with a constrained arc by the HJB approach.

In fig. 10, we show the numerical solution obtained by using the HJB approach. This approach provides also approximations of the optimal final time and the initial costate. Examining the HJB solution also gives an estimate of the bounds for the constrained arc where $y_3 = 1$. The only shooting unknown for which we were not able to obtain relevant information is the multiplier π_{entry} for the costate jump at t_{entry}. Therefore we used $\pi_{entry} = 0.1$ as a starting guess, which turned out to be sufficient for the shooting method to converge properly (Table 8). Fig. 11 shows the corresponding solution, much cleaner than the HJB solution but with the same structure. We checked that the condition $\mu \geq 0$ was satisfied over the boundary arc as p_3 is negative, and $p_3 = 0$ at both entry and exit of the arc as requested by the Hamiltonian continuity conditions. The actual value of the multiplier for the jump on p_3 is $\pi_{entry} = 4.1294$.

	t_f^*	(t_{entry}, t_{exit})	$-\xi^*$ and $p(0)$
Initialization from HJB	7.5	$(1.35, 5.6)$	$(-0.51, -0.24, -0.89, -0.61)$
Solution from PMP	7.0356	$(1.1370, 5.8986)$	$(-0.8672, -0.0474, -0.9860, -0.1667)$

Table 8: (P_4) - Initialization from HJB and solution from PMP.

CPU times. In Table 9 we finally summarize the CPU times needed for computations.

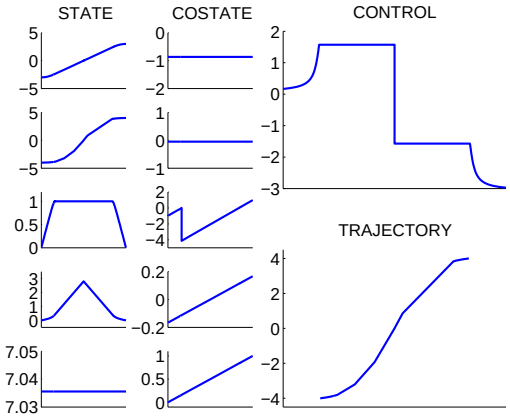

Figure 11: (P_4) - Solution with a constrained arc by PMP approach.

	Problem 1	Problem 2	Problem 3	Problem 4
HJB approach with rough discretization	8×10^{-2}	2.98	211	182
PMP approach with HJB initialization	3×10^{-3}	7×10^{-3}	3×10^{-2}	2×10^{-2}
Shooting function norm for PMP	2.82×10^{-16}	8.14×10^{-11}	1.12×10^{-7}	6.68×10^{-11}

Table 9: Summary of CPU times for numerical experiments (seconds) and shooting function norm

5 Conclusions

The known relation between the gradient of the value function in the HJB approach and the costate in the PMP approach makes it possible to use the HJB results to initialize a shooting method. With this combined method, one can hope to benefit from the optimality of HJB and the high precision of PMP. The main limitation is on the state dimension imposed by HJB.

We have tested this approach on four control problems presenting some specific difficulties: local and global solutions (Problem 1), discontinuous bang-bang control (Problem 2), singular arcs (Problem 3), state constraint (Problem 4). The numerical tests also included two cases where the value function was not differentiable.

For these four problems, the HJB approach provides an approximate solution with some additional information, such as an estimate of the initial costate $p(0)$, optimal final time t_f, structure of the optimal solution with respect to singular or constrained subarcs. In each case this information allowed us to successfully initialize the shooting method. The fact that the optimal control reconstructed by HJB was sometimes far from the exact control did not seem to be problematic for the shooting method initialization. The total computational time for the combined HJB-PMP approach did not exceed four minutes, up to dimension four.

Appendix

Proof of Theorem 3.1. Given the numerical domain Ω we define the set Ω' as

$$\Omega' := \{x \in \mathbb{R}^d \ : \ \widetilde{v}(x;h,\Omega) \leq \min_{x' \in \partial\Omega} \widetilde{v}(x';h,\Omega)\}.$$

The set Ω is the box in which the approximate solution is actually computed and Ω' represents the subset of Ω in which the solution is not affected by the fictitious boundary conditions we need to impose at $\partial\Omega$ to make computation. From the front propagation point of view, $\partial\Omega'$ represents the front at the time it touches $\partial\Omega$ for the very first time.
Let us define $v_{max} := (1 - e^{-\mathcal{T}_{max}})$ and fix $x \in \Omega'$. We have

$$\mathcal{T}(x) \leq \mathcal{T}_{max} < +\infty \quad \text{and} \quad v(x) \leq v_{max} < 1.$$

By (14) we have

$$\widetilde{v}(x;h) \leq v(x) + Ch^\alpha \leq v_{max} + Ch^\alpha.$$

Since $v_{max} < 1$ there exists $h_0 > 0$ such that

$$v_{max} + Ch^\alpha < 1 \quad \text{for all } 0 < h \leq h_0$$

then we can define

$$\widetilde{v}_{max} := v_{max} + Ch_0^\alpha < 1$$

and we have

$$v(x) \leq v_{max} \leq \widetilde{v}_{max} \quad \text{and} \quad \widetilde{v}(x;h) \leq \widetilde{v}_{max} \quad \text{for all } x \in \Omega', \quad 0 < h \leq h_0.$$

For any fixed $x \in \Omega'$, it exists $\xi_x \in [\min\{v(x), \widetilde{v}(x;h)\}, \max\{v(x), \widetilde{v}(x;h)\}]$ such that

$$|\widetilde{\mathcal{T}}(x) - \mathcal{T}(x)| = \Big| \ln\big(1 - v(x)\big) - \ln\big(1 - \widetilde{v}(x;h)\big)\Big| = \left|\frac{1}{1 - \xi_x}\right| |v(x) - \widetilde{v}(x;h)|.$$

Since $\xi_x \leq \widetilde{v}_{max}$, we have

$$|\widetilde{\mathcal{T}}(x) - \mathcal{T}(x)| \leq \frac{Ch^\alpha}{1 - \widetilde{v}_{max}} \quad \text{for all } x \in \Omega' \text{ and } 0 < h \leq h_0$$

and then it exists a positive constant C_2 which depends by the problem's data and on Ω such that

$$\|\widetilde{\mathcal{T}} - \mathcal{T}\|_{L^\infty(\Omega')} \leq C_2 h^\alpha \quad \text{for all } 0 < h \leq h_0. \tag{15}$$

We are now ready to recover an estimate on the gradient of the approximate solution $\widetilde{\mathcal{T}}$. By (15) we know that, for any $i = 1, \ldots, d$

$$\widetilde{\mathcal{T}}(x + ze_i) = \mathcal{T}(x + ze_i) + E_1 \text{ with } |E_1| \leq C_2 h^\alpha$$

and

$$\widetilde{\mathcal{T}}(x - ze_i) = \mathcal{T}(x - ze_i) + E_2 \text{ with } |E_2| \leq C_2 h^\alpha.$$

So we have

$$\widetilde{D}_i\widetilde{\mathcal{T}}(x) = \frac{\mathcal{T}(x + ze_i) + E_1 - (\mathcal{T}(x - ze_i) + E_2))}{2z} = \widetilde{D}_i\mathcal{T}(x) + \frac{E_1 - E_2}{2z}$$

so that

$$|\widetilde{D}_i\widetilde{\mathcal{T}}(x) - \widetilde{D}_i\mathcal{T}(x)| \leq \left|\frac{E_1 - E_2}{2z}\right| \leq C_2\frac{h^\alpha}{z}$$

and then

$$\|\widetilde{D}\widetilde{\mathcal{T}}(x) - \widetilde{D}\mathcal{T}(x)\|_\infty \leq C_2\frac{h^\alpha}{z}.$$

We finally obtain, for $x \in \Omega'$ and $0 < h \leq h_0$,

$$\|\widetilde{D}\widetilde{\mathcal{T}}(x) - D\mathcal{T}(x)\|_\infty \leq \|\widetilde{D}\widetilde{\mathcal{T}}(x) - \widetilde{D}\mathcal{T}(x)\|_\infty + \|\widetilde{D}\mathcal{T}(x) - D\mathcal{T}(x)\|_\infty = O\left(\frac{h^\alpha}{z}\right) + O(z^2)$$

and the conclusion follows. □

References

[1] Bardi, M., Capuzzo Dolcetta, I.: Optimal control and viscosity solutions of Hamilton-Jacobi-Bellman equations. Birkhäuser, Boston (1997)

[2] Bardi, M., Falcone, M., Soravia, P.: Fully discrete schemes for the value function of pursuit-evasion games. In T. Basar and A. Haurie (eds), "Advances in Dynamic Games and Applications", Annals of the International Society of Dynamic Games 1, 89-105 (1994)

[3] Bellman, R. E.: The theory of Dynamic Programming. Bull. Amer. Math. Soc. 60, 503–515 (1954)

[4] Bettiol, P., Frankowska, H.: Normality of the maximum principle for non-convex constrained Bolza problems. J. Differential Equations 243, 256–269 (2007)

[5] Bonnans, F., Martinon, P., Trélat, E.: Singular arcs in the generalized Goddard's problem. J. Optim. Theory Appl. 139, 439–461 (2008)

[6] Bryson, A.E., Ho, Y.-C.: Applied optimal control. Hemisphere Publishing, New-York (1975)

[7] Cannarsa, P., Frankowska, H.: Some characterizations of optimal trajectories in control theory. SIAM J. Control Optim. 28, 1322–1347 (1991)

[8] Cannarsa, P., Frankowska, H., Sinestrari, C.: Optimality conditions and synthesis for the minimum time problem. Set–Valued Analysis 8, 127–148 (2000)

[9] Cernea, A., Frankowska, H.: A connection between the maximum principle and dynamic programming for constrained control problems. SIAM J. Control Optim. 44, 673–703 (2006)

[10] Chitour, Y., Jean, F., Trélat, E.: Genericity results for singular curves. Journal of Differential Geometry, 73, 45–73 (2006)

[11] Clarke, F., Vinter, R.B.: The relationship between the maximum principle and dynamic programming. SIAM J. Control Optim. 25, 1291–1311 (1987)

[12] Deuflhard, P.: Newton Methods for Nonlinear Problems. Springer Series in Computational Mathematics, 35 (2004)

[13] Falcone, M.: Numerical solution of dynamic programming equations. Appendix A in [1].

[14] Falcone, M.: Numerical methods for differential games based on partial differential equations. International Game Theory Review 8, 231–272 (2006)

[15] Gergaud, J., Martinon. P.: Using switching detection and variational equations for the shooting method. Optim. Control Appl. Meth. 28, 95–116 (2007)

[16] Goddard, R.H.: A Method of reaching extreme altitudes. Smithsonian Inst. Misc. Coll. 71, (1919)

[17] Hairer, E., Nørsett, S.P., Wanner, G.: Solving ordinary differential equations I. Springer Series in Computational Mathematics 8, Springer-Verlag, Berlin (1993)

[18] Maurer, H.: Numerical solution of singular control problems using multiple shooting techniques. J. Optim. Theory Appl. 18, 235–257 (1976)

[19] More, J.J., Garbow, B.S., Hillstrom, K.E.: User Guide for MINIPACK-1. Argonne National Laboratory Report ANL-80-74 (1980)

[20] Oberle, H.J.: Numerical computation of singular control functions in trajectory optimization. Journal of Guidance, Control and Dynamics 13, 153–159 (1990)

[21] Pesch, H.J.: A practical guide to the solution of real-life optimal control problems. Control and Cybernetics 23, 7–60 (1994)

[22] Pesch, H.J.: Real-time computation of feedback controls for constrained optimal control problems II: a correction method based on multiple shooting. Optimal Control, Applications and Methods 10, 147-171 (1989)

[23] Pesch, H.J., Plail, M.: The maximum principle of optimal control: a history of ingenious idea and missed opportunities. to appear in Control and Cybernetics.

[24] Pontryagin, L.S., Boltyanski, V.G., Gamkrelidze, R.V. Mishtchenko, E.F.: The mathematical theory of optimal processes. Wiley Interscience, New York (1962)

[25] Seywald, H., Cliff, E.M.: Goddard problem in presence of a dynamic pressure limit. Journal of Guidance, Control, and Dynamics 16, 776–781 (1993)

[26] Soravia, P.: Estimates of convergence of fully discrete schemes for the Isaacs equation of pursuit-evasion differential games via maximum principle. SIAM J. Control Optim. 36, 1–11 (1998)

[27] Tsai, Y.R., Cheng, L.T., Osher, S., Zhao, H.: Fast sweeping algorithms for a class of Hamilton-Jacobi equations. SIAM J. Numer. Anal. 41, 673–694 (2003)

[28] Tsiotras, P., Kelley, H.J.: Drag-law effects in the Goddard problem. Automatica 27, 481-490 (1991)

Centre de recherche INRIA Saclay – Île-de-France
Parc Orsay Université - ZAC des Vignes
4, rue Jacques Monod - 91893 Orsay Cedex (France)

Centre de recherche INRIA Bordeaux – Sud Ouest : Domaine Universitaire - 351, cours de la Libération - 33405 Talence Cedex
Centre de recherche INRIA Grenoble – Rhône-Alpes : 655, avenue de l'Europe - 38334 Montbonnot Saint-Ismier
Centre de recherche INRIA Lille – Nord Europe : Parc Scientifique de la Haute Borne - 40, avenue Halley - 59650 Villeneuve d'Ascq
Centre de recherche INRIA Nancy – Grand Est : LORIA, Technopôle de Nancy-Brabois - Campus scientifique
615, rue du Jardin Botanique - BP 101 - 54602 Villers-lès-Nancy Cedex
Centre de recherche INRIA Paris – Rocquencourt : Domaine de Voluceau - Rocquencourt - BP 105 - 78153 Le Chesnay Cedex
Centre de recherche INRIA Rennes – Bretagne Atlantique : IRISA, Campus universitaire de Beaulieu - 35042 Rennes Cedex
Centre de recherche INRIA Sophia Antipolis – Méditerranée : 2004, route des Lucioles - BP 93 - 06902 Sophia Antipolis Cedex

Éditeur
INRIA - Domaine de Voluceau - Rocquencourt, BP 105 - 78153 Le Chesnay Cedex (France)
http://www.inria.fr
ISSN 0249-6399